Boron Insertion into the N≡N bond of a Tungsten Dinitrogen Complex

Lisa C. Haufe,[†,‡,§] Lukas Endres,[†,‡,§] Merle Arrowsmith,[†,‡] Rüdiger Bertermann,[†,‡] Maximilian Dietz,[†,‡] Felipe Fantuzzi,[¶,*] Maik Finze,[†,‡] Holger Braunschweig[†,‡,**]

[†] Institute for Inorganic Chemistry, Julius-Maximilians-Universität Würzburg, Am Hubland, 97074 Würzburg, Germany. [‡] Institute for Sustainable Chemistry & Catalysis with Boron, Julius-Maximilians-Universität Würzburg, Am Hubland, 97074 Würzburg, Germany. [¶] School of Chemistry and Forensic Science, University of Kent, Canterbury, Park Wood Rd, CT2 7NH, United Kingdom.

ABSTRACT: The 1,3-addition of 1,2-diaryl-1,2-dibromodiboranes ($B_2Ar_2Br_2$) to *trans*-[$W(N_2)_2(dppe)_2$] (dppe = κ^2-($Ph_2PCH_2)_2$), which is accompanied by a Br-Ar substituent exchange between the two boron atoms, is followed by a spontaneous rearrangement of the resulting tungsten diboranyldiazenido complex to a 2-aza-1,3-diboraallenylimino complex displaying a linear, cumulenic B=N=B moiety. This rearrangement involves the splitting of both the B–B and N=N bonds of the N_2B_2 ligand, formal insertion of a BAr boranediyl moiety into the N=N bond and coordination of the remaining BArBr boryl moiety to the terminal nitrogen atom. DFT calculations show that the reaction proceeds via a cyclic NB_2 intermediate, followed by dissociation into a tungsten nitrido complex and a linear boryliminoborane, which recombine by adduct formation between the nitrido ligand and the electron-deficient iminoborane boron atom. The linear B=N=B moiety also undergoes facile 1,2-addition of Brønsted acids (HY = HOPh, HSPh, H_2NPh) with concomitant Y-Br substituent exchange at the terminal boron atom, yielding cationic (borylamino)borylimino tungsten complexes.

Introduction

The reaction of N_2 and H_2 to NH_3 *via* the Haber-Bosch process is the starting point for all synthetic nitrogen-containing compounds, from fertilizers to fine chemicals and pharmaceuticals. Due to the high pressures (150-300 bar) and temperatures (400-500 °C) required it accounts for 1.4% of global CO_2 emissions and 1-2% of the world's total energy consumption. Furthermore, the production of the H_2 required for this process is heavily reliant on fossil fuels.[1,2] In recent years considerable efforts have been undertaken to make ammonia production from N_2 more sustainable, including the design of new hetero- and homogenous catalysts, integrated electro- and photocatalytic processes, and even biological ammonia production.[1-8]

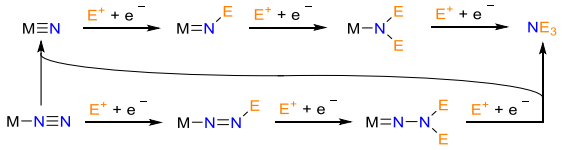

Scheme 1. Typical mechanisms for N_2 functionalization at a metal center.

Another strategy consists of cutting out the NH_3 production step altogether by transforming N_2 directly into value-added nitrogen-containing small molecules. Since the synthesis of the first stable terminal dinitrogen complex, $[Ru(NH_3)_5N_2]^{2+}$, by Allen and Senoff nearly 60 years ago,[9] a wide variety of transition metal complexes with N_2 ligands in various coordination modes have been reported,[10-13] some capable of spontaneously splitting the N≡N triple bond to form nitride complexes.[14] Many of these complexes have been used as versatile platforms for the direct stoichiometric formation of N–C, N–Si, N–B, N–Al and N–P bonds from N_2, with or without splitting the dinitrogen N–N bond.[15-20] Furthermore, several systems have been successfully employed for the catalytic synthesis of tertiary and secondary silylamines[21-25] and, most recently, tertiary borylamines[26] from N_2 under highly reducing conditions.

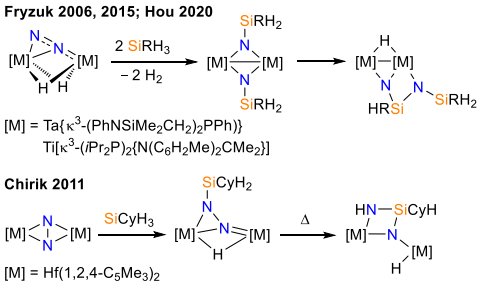

Scheme 2. Formation of NSiRHN(SiRH) ligands by insertion of SiRH units into the N–N bond of metal dinitrogen complexes.

While the majority of N_2 functionalization reactions at transition metals result in either terminal functionalization with retention of the N–N bond or splitting of the N–N bond into two nitride moieties followed by functionalization of each separate nitrogen atom (Scheme 1), there have been very few examples of insertion of a heteroatom between the two nitrogen atoms of metal-bound N_2 (Scheme 2). Fryzuk and co-workers reported that (μ-η^1:η^2-N_2)-bridged tantalum hydride dimers supported by NPN pincer ligands first react with two molar equivalents of Si*t*BuH$_3$ or Si*n*BuH$_3$ to form bis(silylnitrene)-bridged tantalum dimers, which rearrange into κ^2-(μ-N-Si*t*BuHN)Si*t*BuH-bridged complexes, the reaction being accompanied by additional dehydrocoupling and ligand C–H activation in the case of the phenylphosphino-PNP complex.[27,28] More recently, Hou observed very similar reactivity between two equivalents Si-PhH$_3$ and a (μ-η^1:η^2-N_2)-bridged PNP-titanium hydride dimer.[29]

Chirik also reported the insertion of a SiCyH unit into the N–N bond of a (μ^2,η^2,η^2-N_2)-bridged hafnocene dimer, generating a κ^2-(μ-N-SiCyHNH) ligand *via* consecutive 1,3- and 1,2-hydrosilylation steps.[30] In all these cases the electrons required for splitting the N≡N bond all come from the two metal centers.

Building on earlier works by Komiya, Szymczak and Ashley on the end-on N_2 functionalization of [Fe(N_2)(depe)$_2$] (depe = κ^2-(Et_2PCH_2)$_2$) with silyl and boryl groups,[31-33] and a report by Hiroshige *et al.* on the first borylation of a tungsten dinitrogen complex,[34] our own group and that of Simonneau have reported the 1,3-functionalization of *trans*-[W(N_2)$_2$(depe)$_2$] and *trans*-[M(N_2)$_2$(dppe)$_2$] (M = Mo, W; dppe = κ^2-(Ph_2PCH_2)$_2$) with borane and diborane precursors (Scheme 3).[35-40] Herein we present the 1,3-bromodiboranylation of *trans*-[W(N_2)$_2$(dppe)$_2$] with 1,2-diaryl-1,2-dibromodiboranes(4), followed by spontaneous rearrangement with insertion of a BAr unit between the two nitrogen atoms of the diazenido ligand, the first example of such an insertion at a monometallic dinitrogen complex. In this case two of the electrons required for splitting the N≡N bond come from the diborane precursor. The electronic structure of these systems has been studied in detail, along with mechanistic investigations using density functional theory (DFT) and high-level coupled-cluster calculations.

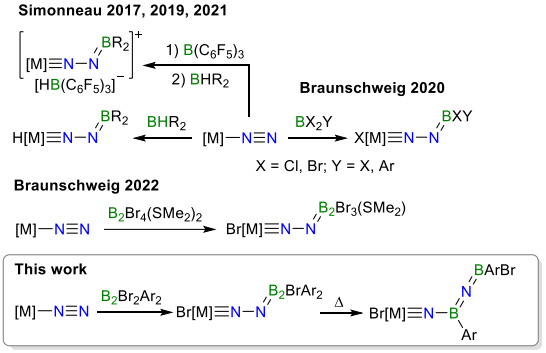

Scheme 3. Reactions of group 6 complexes of the form [M(N_2)$_2${(R_2PHC_2)$_2$}$_2$] (M = Mo, W; R = Et, PH) with boranes and diboranes.

Results and Discussion

The addition of 1.3 equivalents of $B_2Br_2Mes_2$ (Mes = 2,4,6-trimethylphenyl) to *trans*-[W(N_2)$_2$(dppe)$_2$] resulted in the formation of a dark brown solution, accompanied by evolution of N_2. After 2 h stirring at rt, complex **1-Mes**, which results from the 1,3-diboranylation of the WN_2 unit concomitant with Br-Mes substituent exchange at the B_2 unit, was precipitated by the addition of pentane as a brown-golden solid (94% yield, Scheme 4a). While the solution ^{11}B NMR spectrum of **1-Mes** was silent (as has often been observed for the boryl- and diboranyldiazenido complexes displayed in Scheme 3),[39-40] solid-state ^{11}B NMR spectroscopy showed two broad resonances at 87.0 (NB*B*) and 19.0 (N_2*B*) ppm. NMR shift calculations on **1-Mes** at the ωB97X-D/Def2-TZVP level of theory, using 1,2-dibromo-1,2-bis(dimethylamino)diborane(4) ($B_2Br_2(NMe_2)_2$, δ_{11B} = 38 ppm) as a reference,[41] provided similar shifts of 80.0 and 23.6 ppm for the terminal and internal boron atoms, respectively. The ^{31}P NMR spectrum showed a new singlet at 39.8 ($^1J_{WP}$ = 288 Hz), slightly upfield from previously published diboranyldiazenido complexes (δ_{31P} = 33-39 ppm).[40] The IR spectrum of **1-Mes** showed a strong stretching band at 1569 cm^{-1} (ν(N=N)$_{calcd}$ = 1570 cm^{-1} at the ωB97X-D/Def2-SVP level of theory), at slightly higher wavenumber than the range observed for diboranyldiazenido complexes (1528 to 1550 cm^{-1}).[40] This higher wavenumber indicates a slightly stronger N=N bond in **1-Mes** compared to those of similar diboranyldiazenido complexes. X-ray crystallographic analysis finally confirmed the structure of **1-Mes** and the exchange of the mesityl and bromide substituents between the internal and terminal boron atoms.[42]

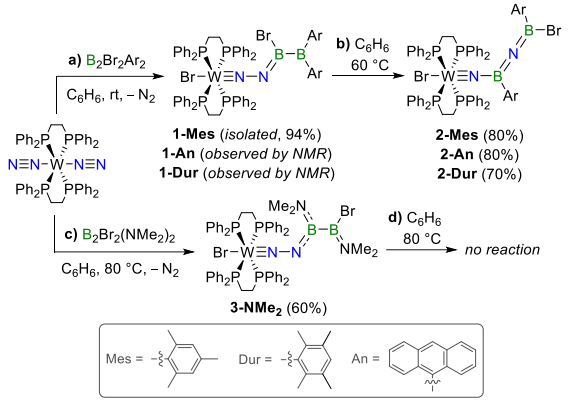

Scheme 4. Reactions of **(a,b)** 1,2-diaryl-1,2-dibromodiboranes(4) and **(c)** 1,2-bis(dimethylamino)-1,2-dibromodiborane(4) with *trans*-[W(N_2)$_2$(dppe)$_2$].

Heating a benzene solution of **1-Mes** at 60 °C for 15 h or performing the reaction of $B_2Br_2Mes_2$ and *trans*-[W(N_2)$_2$(dppe)$_2$] at 60 °C led to an unexpected quantitative rearrangement to complex **2-Mes**, in which one BMes moiety had inserted into the N–N double bond, resulting in a terminal NB(Mes)NB(Br)Mes ligand (Scheme 4b). The complex and broad solid-state ^{11}B NMR signal was modelled to three components with isotropic chemical shifts of 30.0, 29.2 and 19.3 ppm. Calculations indicate that these correspond to two atropisomers of **2-Mes**, differing by a 180° rotation of the BBrMes moiety around the terminal N=B multiple bond. Rotamer 1, which corresponds to the solid-state structure in Fig. 1 ($\delta_{11B\text{-}calcd}$ = 28.5 (N*B*N), 17.9 (N*B*) ppm) is 4.2 kcal mol^{-1} more stable than rotamer 2 ($\delta_{11B\text{-}calcd}$ = 26.8 (N*B*N), 18.2 (N*B*) ppm, see Fig. S77 in the SI). The ^{31}P{^{1}H} NMR resonance of **2-Mes** (28.7 ppm) is upfield-shifted by ca. 10 ppm compared to that of **1-Mes** and broadened by fluxional processes in solution (fwmh ≈ 340 Hz). Above 70 °C the ^{31}P{^{1}H} NMR signal sharpens into a narrow singlet at 31.1 ppm ($^1J_{WP}$ = 298 Hz), indicating free rotation of the NBNB ligand around the W–N bond. Upon cooling below –10 °C the ^{31}P{^{1}H} NMR signal broadens considerably until it splits below –50 °C into four 1:1:1:1 doublet of doublets of doublets at 38.8, 29.9, 19.2 and 13.8 ppm, freezing out rotamer 1.

The solid-state structure of **2-Mes** confirms the cleavage of, and insertion of a BMes moiety into, the N–N bond, while the terminal boron atom now bears a bromide and the second Mes substituent (Figure 1 and Table 1). The W1–N1 distance of 1.7655(16) is shorter than those of neutral boryl- and diboranyldiazenido complexes (1.77-1.81 Å),[31-40] indicating an increase in its double bond character.

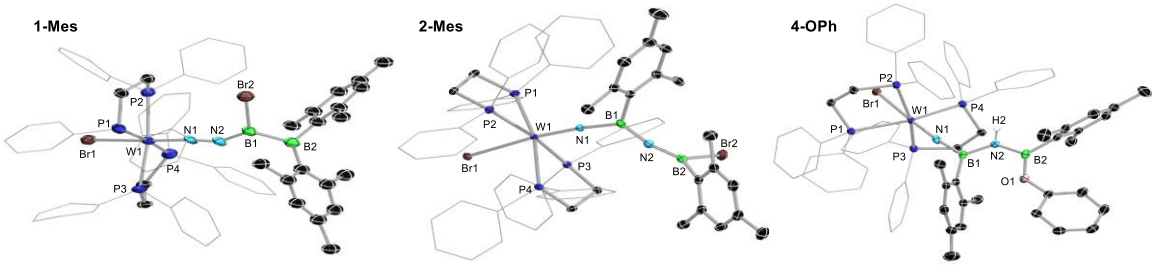

Figure 1. Crystallographically-determined solid-state structures of **1-Mes**, **2-Mes** and **4-OPh** (Br^- counteranion omitted). Thermal displacement ellipsoids at 50%. Ellipsoids of dppe phenyl groups and hydrogen atoms omitted for clarity, except for N2-bound H2 in **4-OPh**.

Table 1. Selected bond lengths (Å) and angles (°) for crystallographically characterized **2-Ar** (Ar = Mes, An, Dur), **3-NMe$_2$**, **4-OPh** and **5-NHPh**.

	W1–N1	N1–B1	B1–N2	N2–B2	B2–Y	W1-N1-B1	N1-B1-N2	B1-N2-B2	B1∠B2
2-Mes	1.7655(16)	1.519(3)	1.361(3)	1.331(3)	–	173.76(13)	121.04(18)	162.05(19)	87.5
2-An	1.753(6)	1.512(11)	1.371(12)	1.349(13)	–	172.0(6)	121.6(8)	161.0(9)	79.3
2-Dur	1.7576(16)	1.516(3)	1.360(3)	1.327(3)	–	173.87(14)	119.21(18)	158.9(2)	83.0
4-OPh	1.772(2)	1.482(4)	1.426(4)	1.449(4)	1.360(4)[a]	170.51(18)	117.7(2)	131.2(2)	7.6
5-NHPh	1.730(6)	1.483(9)	1.407(10)	1.466(12)	1.409(11)[b]	164.0(5)	112.9(6)	135.2(7)	7.0
	W1–N1	N1–N2	N2–B1	B1–B2	B1–N3	B2–N4	W1-N1-N2	N1-N2-B1	N2-B1-B2
3-NMe$_2$	1.827(4)	1.213(5)	1.449(7)	1.715(8)	1.418(7)	1.374(7)	174.9(3)	142.2(4)	124.7(5)

[a] Y = O1; [b] Y = N3.

The B1–N1 bond (1.519(3) Å), which shows slight double bond character, is significantly longer than the B1–N2 and N2–B2 bonds (1.361(3) and 1.331(3) Å, respectively), the latter both showing strong double bond character.[43,44] Compared to the related octahedral bis(borylimido)tungsten complex [W(NBMes)$_2$Cl$_2$(PMe$_3$)$_2$] (avg. W–N 1.78, N–B 1.44 Å; avg. W-N-B 176°),[45] the W–N bond in **2-Mes** is slightly shorter, while the N1–B1 bond is significantly longer, owing to the additional π donation from N2 to B1. The two trigonal planar boron centers are orthogonal to each other (B1∠B2 87.5°). With its near-linear B1-N2-B2 unit (162.05(19)°), which is isostructural and isoelectronic to an allenyl fragment, the NBNB ligand can be described as a η^1-(2-aza-1,3-diboraallenyl)imido ligand. Only two compounds with a similar linear >B=N=B< unit have been crystallographically authenticated to date, namely the [Mes$_2$B=N=BMes$_2$]$^-$ anion and a neutral N-heterocyclic carbene (NHC)-stabilized species of the form [(NHC)ArB=N=B(BNAr')R], both showing similar structural features (B–N 1.34-1.36 Å; B-N-B 163-176°) to **2-Mes**.[46,47] The solid-state IR spectrum of **2-Mes** showed a strong, broad stretching band at 1667 cm^{-1} for the B=N=B bonding motif, similar to that observed by Nöth for the [*t*Bu$_2$B=N=B*t*Bu$_2$]$^-$ anion (1660-1690 cm^{-1}).[48]

The room-temperature reaction of *trans*-[W(N$_2$)$_2$(dppe)$_2$] and B$_2$Br$_2$An$_2$ (An = 9-anthryl) in benzene also proceeded in an analogous fashion. While the 1,3-bromodiboranylation product **1-An** was observed by solution NMR spectroscopy (δ_{31P} = 38.3 (s, $^1J_{WP}$ = 287 Hz) ppm) it converted too rapidly to **2-An** (δ_{31P} = 33.9 ppm) to enable its isolation (Scheme 4a,b). At 60 °C complete conversion to **2-An** was achieved in 40 min. Under the same conditions the more sterically demanding B$_2$Br$_2$Dur$_2$ (Dur = 2,3,5,6-tetramethylphenyl) underwent quantitative conversion to **2-Dur** (δ_{31P} = 30.0 (br) ppm) within 80 min. The intermediate **1-Dur** was observed by ^{31}P NMR spectroscopy at 40.4 ppm. **2-An** and **2-Dur** were isolated as beige and brown crystalline solids, respectively, in yields of 80% and 70%, respectively. Their solid-state structures (see Figs. S72-S73 in the SI), like that of **2-Mes**, show a slightly distorted octahedral tungsten(IV) complex bearing an η^1-(2-aza-1,3-diboraallenyl)imido ligand with a conjugated B1-N2-B2 unit (avg. B1–N2 ca. 1.364 Å; N2–B2 ca. 1.336 Å) approaching linearity (avg. B-N-B 160.7°). It is noteworthy that the reaction of B$_2$Br$_2$(NMe$_2$)$_2$ with *trans*-[W(N$_2$)$_2$(dppe)$_2$] yielded the simple 1,3-bromodiboranylation product **3-NMe$_2$** (δ_{11B} = 41.7 (*B*BrNMe$_2$), 25.2 (N$_2$*B*Br) ppm) without migration of the Br and NMe$_2$ ligands (Scheme 4c). Furthermore, **3-NMe$_2$** did not undergo insertion of a boryl moiety into the N–N bond even under forcing conditions (Scheme 4d).

To elucidate the driving force behind boron insertion into the N≡N bond, we conducted a detailed investigation of the intricate rearrangement mechanism from **1-Mes** to **2-Mes** using quantum chemical calculations (see full details of the methodology and calculations in the SI). Due to the computational demands associated with handling the full **1-Mes** molecule and related systems, all including multiple aromatic substituents, we employed a QM/QM approach for geometric optimizations. Specifically, the phenyl groups attached to the diphosphine ligands were treated with the computationally cheaper semi-empirical PM7 level of theory, incorporating Grimme's D3 empirical dispersion and Becke-Johnson damping. The remainder of the system was described by DFT calculations at the ωB97X-D/Def2-SVP level of theory.

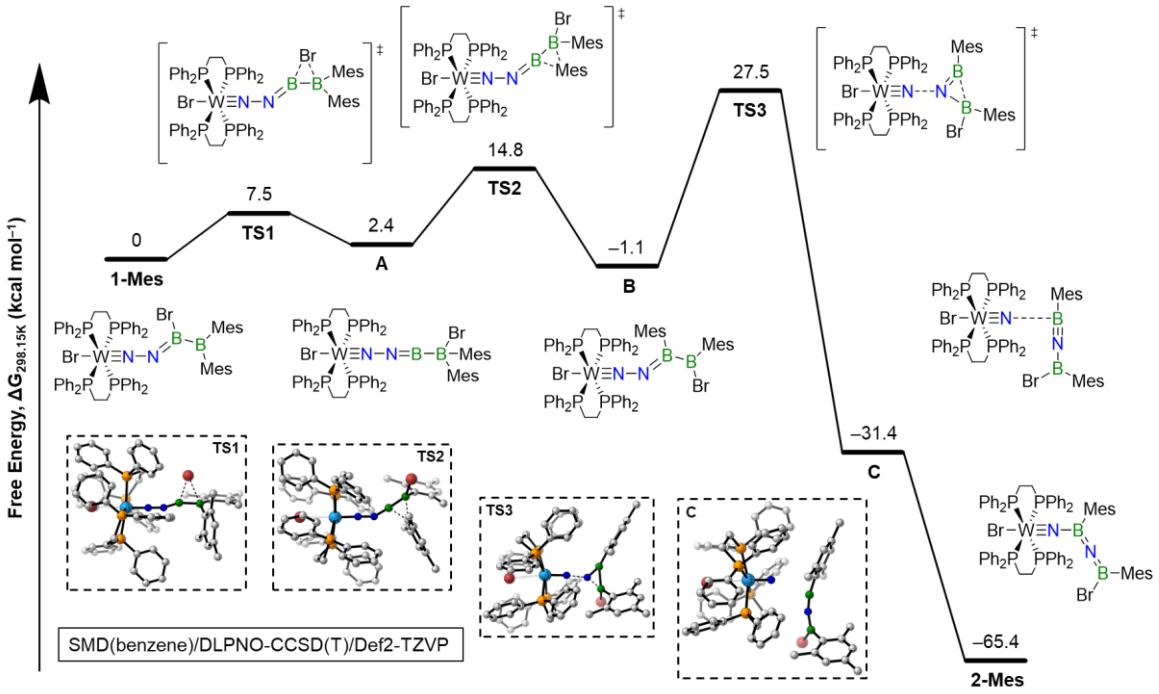

Figure 2. Free energy profile (kcal mol^{-1}) of the proposed mechanistic pathway for the formation of the boron insertion product **2-Mes** from **1-Mes**. Energies are referenced to **1-Mes** and calculated at the SMD(benzene)/DLPNO-CCSD(T)/Def2-TZVP level of theory. The 3D structures of **TS1**, **TS2**, **TS3**, and **C** are also shown. Hydrogen atoms are omitted for clarity.

This approach strikes a balance between computational efficiency and accuracy as the bulky diphosphine ligands primarily contribute to the rearrangement mechanism through steric effects. For a more accurate determination of the relative Gibbs free energies single-point calculations on the optimized structures were performed at the SMD(benzene)/DLPNO-CCSD(T)/Def2-TZVP level. To ensure the proper connectivity between corresponding energy minima in the reaction mechanism all transition states were analyzed through intrinsic reaction coordinate (IRC) calculations (see Figs. S78-S80 in the SI). Our computed reaction mechanism is shown in Figure 2 (see SI for further details).

The formation of **1-Mes** from *trans*-[W(N$_2$)$_2$(dppe)$_2$] and B$_2$Br$_2$Mes$_2$ under release of N$_2$ is highly exergonic (ΔG = –42.7 kcal mol^{-1}). Starting from **1-Mes** and progressing to intermediate **B** an exchange occurs involving one of the mesityl groups at the terminal boron atom and the bromine atom of the neighboring boron. This exchange unfolds in two sequential steps. Initially, the bromine atom shifts to the terminal boron atom via **TS1**, leading to the formation of intermediate **A**, which adopts a linear NNB(sp^1)B(sp^3) geometry. This conformation is remarkably stable, with **A** being only ΔG = 2.4 kcal mol^{-1} above **1-Mes**. The migration of the mesityl group from **A** to **B** follows a similar path via **TS2**. Both migrations at **TS1** and **TS2** occur readily at room temperature thanks to their low barriers of only 7.5 and 14.8 kcal mol^{-1}, respectively. The resulting intermediate **B** is slightly favored with ΔG = –1.1 kcal mol^{-1} compared to **1-Mes**. It is noteworthy, however, that this minor preference may be attributable to numerical artifacts, as both **1-Mes** and **B** could possess distinct but energetically closely situated rotamers. This could explain why **B**, which should be formed first in the reaction of [W(N$_2$)$_2$(dppe)$_2$] with B$_2$Br$_2$Mes$_2$, is never observed experimentally. The exchange of the bromide and aryl substituents at the diboron unit is reminiscent of the inorganic Wagner-Meerwein-type rearrangement observed upon coordination of a single Lewis base (L = phosphine, carbene) to B$_2$Ar$_2$X$_2$ (X = Cl, Br, I; Ar = Mes, Dur).[49,50] Here, the terminal N$_2$ ligand likely acts as the Lewis base, coordinating to one boron atom and inducing the Ar-Br rearrangement.

Proceeding from **B**, the formation of **TS3** occurs as the rate-determining step of the rearrangement from **1-Mes** to **2-Mes**. Here, an asymmetric three-membered B$_2$N ring forms from the rotation around the N-N-B-B dihedral angle with N–B distances of 1.32 and 1.46 Å. Furthermore, the N–N bond length expands to 1.72 Å. **TS3** is 28.6 kcal mol^{-1} above intermediate **B**, which is not readily attainable at room temperature but becomes feasible at the elevated reaction temperature of 60 °C. The formation of the B$_2$N ring in **TS3** also explains the lack of rearrangement in **3-NMe$_2$** as the terminal boron atom B2 is already electronically saturated by the π-donating dimethylamino group, thus making donation from N2 to the terminal boron atom B2 unfavorable.[51]

Subsequently, the N–N bond is fully cleaved, followed by insertion of a single nitrogen atom into the B–B bond. This leads to the formation of a van der Waals complex featuring the iminoborane [Br(Mes)B–N≡BMes] and the tungsten nitride complex [(Br)W(N)(dppe)$_2$] (**C**). The latter was isolated in 1982 by the group of Leigh,[52] and thus represents a credible intermediate in the transformation of **1-Mes** to **2-Mes**. The interaction within the van der Waals complex occurs between the sp^1-boron atom and the tungsten-bound nitrogen atom (WN···B 3.11 Å), this distance being smaller than the sum of the van der Waals radii (3.47 Å). Formation of the product **2-Mes** then occurs via the recoupling of the fragments through B–N bond formation between these two atoms. Relaxed energy scans following this bond coordinate did not point to the existence of a kinetic barrier between **C** and **2-Mes**. The last two steps occur through

highly exergonic reactions of –58.9 and –34.0 kcal mol^{-1}, respectively, with **2-Mes** located at ΔG = –65.4 kcal mol^{-1} with respect to **1-Mes**.[53]

To assess the bonding situation of **2-Mes**, we conducted calculations of Mayer bond orders (MBOs) and intrinsic bonding orbitals (IBOs). These calculations suggest the presence of a W≡N triple bond and a cumulene-type bonding configuration for the linear B=N=B segment of the system. The corresponding MBOs are 2.57 (W≡N), 1.71 (B=N) and 1.69 (N=B), respectively. This picture is fully supported by IBO calculations (Figure 3).

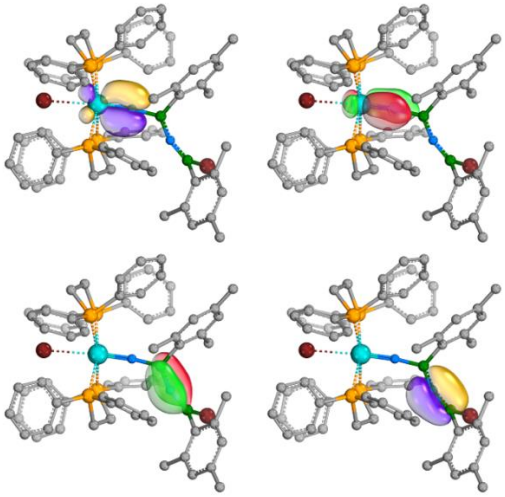

Figure 3. IBOs for the π space of the W–N (top) and B–N–B (bottom) bonding motifs of **2-Mes**. Hydrogen atoms are omitted for clarity.

To test the reactivity of the conjugated, linear B=N=B moiety, **2-Mes** was combined with various Brønsted acids. Phenol, thiophenol and aniline all reacted at room temperature with **2-Mes** to yield the colorless ionic 1,2-addition products **4-Y** (Y = OPh, SPh, NHPh), in which the terminal bromide ligand has been displaced and the Y–H bond added across the B2–N2 bond (Scheme 5a). The solution ^{11}B NMR spectra of **4-Y** showed no resonances, presumably due to excessive line-broadening. A solid-state ^{11}B NMR spectrum of **4-OPh** provided shifts of 41.0/35.4 (two rotamers) and 20.1 ppm for the terminal and internal boron nuclei, respectively. The ^{31}P NMR spectra showed a singlet in the 31-33 ppm range ($^{1}J_{WP}$ = 290 Hz), down-field-shifted from **2-Mes** (δ_{31P} = 28.7 ppm). The ^{1}H NMR B$_2$N*H* proton resonance is observed in the 4.5-5.4 ppm range, shifting further upfield as the electron-donating ability of Y decreases.

The solid-state structure of **4-OPh** further confirms the 1,2-addition across the terminal B–N bond. The NBNBO framework is quasi planar (torsion angles N1-B1-N2-B2 –177.9(3), B1-N2-B2-O1 4.7(4)°), with the NH and BOPh functionalities in a *trans* conformation across the B2–N2 bond. The B1–N2 and N2–B2 bond lengths of 1.426(4) and 1.449(4) Å, respectively, are considerably longer than those in **2-Mes** (B1–N2 1.361(3), B2–N2 1.331(3) Å), as expected upon switching from sp^1 to sp^2 hybridization for the internal nitrogen atom. **4-NHPh** was slowly oxidized in dichloromethane to the neutral tungsten(VI) complex **5-NHPh** (δ_{31P} = 39.7 ppm), in which the tungsten-bound bromide and one dppe ligand have been replaced by three chloride ligands (Scheme 5b).

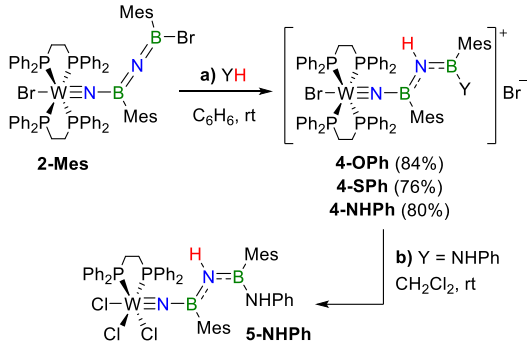

Scheme 5. Reactions of **2-Mes** with protic reagents.

The solid-state structure of **5-NHPh** confirms the 1,2-addition of the aniline N–H bond across the terminal B2–N2 bond, the NH and BNHPh functionalities being in a *trans* conformation. The NBNBN framework is quasi-planar (torsion angles N1-B1-N2-B2 –169.4(8), B1-N2-B2-N3 –6.2(15)°), with relatively short B1–N2 and B2–N3 bonds (1.407(10), 1.409(11) Å) and a slightly longer N2–B2 bond (1.466(12) Å), all within the range of partial double bonds. Similar oxidation processes were also observed for **4-OPh** and **4-SPh** in CH_2Cl_2, albeit at a slower rate (see Figs. S54-S56 in the SI).

Conclusions

We have shown that tungsten diboranyldiazenido complexes, formed by the 1,3-bromoboration of *trans*-[W(N$_2$)$_2$(dppe)$_2$] with a diaryl(dibromo)diborane(4) (B$_2$Br$_2$Ar$_2$) rearrange under very mild reaction conditions by insertion of one boron atom into the N=N bond and Br-Ar ligand exchange between the boron atoms of to a 2-aza-1,3-diboraallenylimino complex displaying a linear cumulenic B=N=B moiety. A theoretical mechanistic study shows that the reaction proceeds via a cyclic NB$_2$ transition state, leading to an intermediate boryliminoborane and tungsten nitride complex, which recombine by adduct formation between the nitride ligand and the electron-deficient iminoborane boron atom. This last step provides a platform for expanding this chemistry to the N-functionalization of other transition-metal nitride complexes with iminoboranes. Room-temperature reactions of the B=N=B moiety with various protic reagents (HY) resulted in protonation of the central nitrogen atom and Br-Y ligand exchange at the terminal boron atom, providing cationic (borylamino)borylimino tungsten complexes. The end-on addition to, and insertion into, a metal-bound dinitrogen ligand of a boryl (BArBr) and a boranediyl (BAr) moiety, combined with the subsequent 1,2-addition of protic reagents to the resulting allenic B=N=B functionality, provides the first example of tandem dinitrogen splitting/borylation incorporating both nitrogen atoms into the same product.

ASSOCIATED CONTENT

The Supporting Information is available free of charge at https://pubs.acs.org/doi/10.1021/jacs.xxxxxx

Experimental Section, plots of NMR, UV-vis and IR spectra for new compounds, and complete details of crystallographic experiments and computational calculations (PDF).

Accession codes.

CCDC 2268262 (**2-Dur**), 2268263 (**4-OPh**), 2268264 (**2-An**), 2268265 (**2-Mes**), 2268266 (**3-NMe$_2$**), 2268267 (**5-NHPh**) and 2268268 (**1-Mes**) contain the supplementary crystallographic data for this paper. These data can be obtained free of charge via

www.ccdc.cam.ac.uk/data_request/cif, or by emailing data_request@ccdc.cam.ac.uk, or by contacting The Cambridge Crystallographic Data Centre, 12 Union Road, Cambridge CB2 1EZ, UK; fax: +44 1223 336033.

AUTHOR INFORMATION

Corresponding Author

* F.Fantuzzi@kent.ac.uk
** H.Braunschweig@uni-wuerzburg.de.

ORCID

Merle Arrowsmith: 0000-0003-1449-5932
Holger Braunschweig: 0000-0001-9264-1726
Felipe Fantuzzi: 0000-0002-8200-8262
Maik Finze: 0000-0002-6098-7148

Author contributions

§ L.H. and L.E. contributed equally.

Notes

The authors declare no competing financial interest.

ACKNOWLEDGMENTS

Financial support from the Deutsche Forschungsgemeinschaft (DFG, German Research Foundation) is gratefully acknowledged (project number 466754611). L. M. thanks the Verband der Chemischen Industrie (VCI) for a Kekulé fellowship.

REFERENCES

(1) Wang, M.; Khan, M. A.; Mohsin, I.; Wicks, J.; Ip, A. H.; Sumon, K. Z.; Dinh, C.-T.; Sargent, E. H.; Gates, I. A.; Kibria, M. G. Can sustainable ammonia synthesis pathways compete with fossil-fuel based Haber-Bosch processes? *Energy Environ. Sci.* **2021**, *14*, 2535–2548.

(2) Smith, C.; Hill, A. K.; Torrente-Murciano, L. Current and future role of Haber–Bosch ammonia in a carbon-free energy landscape. *Energy Environ. Sci.* **2020**, *13*, 331–344.

(3) Marakatti, V. S.; Gaigneaux, E. M. Recent Advances in Heterogeneous Catalysis for Ammonia Synthesis. *ChemCatChem* **2020**, *12*, 5838–5857.

(4) Ghavam, S.; Vahdati, M.; Wilson, I. A. G.; Styring, P. Sustainable Ammonia Production Processes. *Front. Energy Res.* **2021**, *9*, Article 580808.

(5) Soloveichik, G. Electrochemical synthesis of ammonia as a potential alternative to the Haber-Bosch process. *Nature Catal.* **2019**, *2*, 377–380.

(6) Qi, P.; Gao, X.; Wang, J.; Liu, H.; He, D.; Zhang, Q. A minireview on catalysts for photocatalytic N_2 fixation to synthesize ammonia. *RSC Adv.* **2022**, *12*, 1244–1257.

(7) Zheng, J.; Jiang, L.; Lyu, Y.; Jiang, S. P.; Wang, S. Green Synthesis of Nitrogen-to-Ammonia Fixation: Past, Present, and Future. *Energy Environ. Mater.* **2022**, *5*, 452–457

(8) Watanabe, Y.; Aoki, W.; Ueda, M. Sustainable Biological Ammonia Production towards a Carbon-Free Society. *Sustainability* **2021**, *13*, Article 9496.

(9) Allen, A. D.; Senoff, C. V. Nitrogenopentammineruthenium(II) Complexes. *Chem. Commun.* **1965**, 621–622.

(10) Ballmann, J.; Munhé, R. F.; Fryzuk, M. D. The hydride route to the preparation of dinitrogen complexes. *Chem. Commun.* **2010**, *46*, 1013–1025.

(11) Fryzuk, M. D. Side-on End-on Bound Dinitrogen: An Activated Bonding Mode That Facilitates Functionalizing Molecular Nitrogen. *Acc. Chem. Res.* **2009**, *42*, 127–133.

(12) MacLachlan, E. A.; Fryzuk, M. D. Synthesis and Reactivity of Side-On-Bound Dinitrogen Metal Complexes. *Organometallics* **2006**, *25*, 1530–1543.

(13) Burford, R. J.; Fryzuk, M. D. Examining the relationship between coordination mode and reactivity of dinitrogen. *Nature Rev. Chem.* **2017**, *1*, Article 0026.

(14) Forrest, S. J. K.; Schluschaß, B.; Yuzik-Klimova, E. Y.; Schneider, S. Nitrogen Fixation via Splitting into Nitrido Complexes. *Chem. Rev.* **2021**, *121*, 6522–6587.

(15) Masero, F.; Perrin, M. A.; Dey, S.; Mougel, V. Dinitrogen Fixation: Rationalizing Strategies Utilizing Molecular Complexes. *Chem. Eur. J.* **2021**, *27*, 3892–3928.

(16) Kim, S.; Loose, F.; Chirik, P. J. Beyond Ammonia: Nitrogen–Element Bond Forming Reactions with Coordinated Dinitrogen. *Chem. Rev.* **2020**, *120*, 5637–5681.

(17) Simonneau, A. Transition metal-mediated dinitrogen functionalisation with boron. *New J. Chem.* **2021**, 45, 9294–9301.

(18) Lv, Z.-J.; Wei, J.; Zhang, W.-X.; Chen, P.; Deng, D.; Shi, Z.-J.; Xi, Z. Direct transformation of dinitrogen: synthesis of *N*-containing organic compounds via N–C bond formation. *Natl. Sci. Rev.* **2020**, *7*, 1564–1583.

(19) Simonneau, A.; Etienne, M. Enhanced Activation of Coordinated Dinitrogen with p-Block Lewis Acids. *Chem. Eur. J.* **2018**, *24*, 12458–12463.

(20) Khoenkhoen, N.; de Bruin, B.; Reek, J. N. H.; Dzik, W. I. Reactivity of Dinitrogen Bound to Mid- and Late-Transition-Metal Centers. *Eur. J. Inorg. Chem.* **2015**, 567–598.

(21) Walter, M. D. Recent Advances in Transition Metal-Catalyzed Dinitrogen Activation. *Adv. Organomet. Chem.* **2016**, *65*, 261–377.

(22) Kuriyama, S.; Nishibayashi, Y. Development of catalytic nitrogen fixation using transition metal complexes not relevant to nitrogenases. *Tetrahedron* **2021**, *83*, Article 131986.

(23) Tanabe, Y.; Nishibayashi, Y. Recent advances in catalytic silylation of dinitrogen using transition metal complexes. *Coord. Chem. Rev.* **2019**, *389*, 73–93.

(24) Nishibayashi, Y. Development of catalytic nitrogen fixation using transition metal–dinitrogen complexes under mild reaction conditions. *Dalton Trans.* **2018**, *47*, 11290–11297.

(25) Arnold, P. L.; Ochiai, T.; Lam, F. Y. T.; Kelly, R. P.; Seymour, M. L.; Maron, L. Metallacyclic actinide catalysts for dinitrogen conversion to ammonia and secondary amines. *Nature Chem.* **2020**, *12*, 654–659.

(26) Bennaamane, S.; Espada, M. F.; Liao, Q.; Saffon-Merceron, N.; Massou, S.; Clot, E.; Nebra, N.; Fustier-Boutignon, M.; Mézailles, N. Catalytic Reduction of N_2 to Borylamine at a Molybdenum Complex. *Angew. Chem. Int. Ed.* **2018**, *57*, 12865–20214.

(27) MacKay, B. A.; Munha, R. F.; Fryzuk, M. D. Substituent Effects in the Hydrosilylation of Coordinated Dinitrogen in a Ditantalum Complex: Cleavage and Functionalization of N_2. *J. Am. Chem. Soc.* **2006**, *128*, 9472–9483.

(28) Yeo, A.; Shaver, M. P.; Fryzuk, M. D. A New Side-on End-On Ditantalum Dinitrogen Complex and Its Reaction with $BuSiH_3$. *Z. Anorg. Allg. Chem.* **2015**, *641*, 123–127.

(29) Mo, Z.; Shima, T.; Hou, Z. Synthesis and Diverse Transformations of a Dinitrogen Dititanium Hydride Complex Bearing Rigid Acridane-Based PNP-Pincer Ligands. *Angew. Chem. Int. Ed.* **2020**, *59*, 8635–8644.

(30) Semproni, S. P.; Lobkovsky, E.; Chirik, P. J. Dinitrogen Silylation and Cleavage with a Hafnocene Complex. *J. Am. Chem. Soc.* **2011**, *133*, 10406–10409.

(31) Hirano, M.; Akita, M.; Morikita, T.; Kubo, H.; Fukuoka, A.; Komiya, S. Synthesis, structure and reactions of a dinitrogen complex of iron(0), $[Fe(N_2)(depe)_2]$ (depe = $Et_2PCH_2CH_2PEt_2$). *J. Chem. Soc., Dalton Trans.* **1997**, 3453–3458.

(32) Geri, J. B.; Shanahan, J. P.; Szymczak, N. K.Testing the Push–Pull Hypothesis: Lewis Acid Augmented N_2 Activation at Iron. *J. Am. Chem. Soc.* **2017**, 139, 5952–5956.

(33) Piascik, A. D.; Hill, P. J.; Crawford, A. D.; Doyle, L. R.; Green, J. C.; Ashley, A. E. Cationic silyldiazenido complexes of the

Fe(diphosphine)$_2$(N_2) platform: structural and electronic models for an elusive first intermediate in N_2 fixation. *Chem. Commun*. **2017**, *53*, 7657–7660.

(34) Hiroshige, I.; Youichi, I.; Masanobu., H. Synthesis of Boryldiazenido Complexes from Tungsten Dinitrogen Complexes. *Chem. Lett*. **1998**, *27*, 677–678.

(35) Coffinet, A.; Specklin, D.; Vendier, L.; Etienne, M.; Simonneau, A. Frustrated Lewis Pair Chemistry Enables N_2 Borylation by Formal 1,3-Addition of a B–H Bond in the Coordination Sphere of Tungsten. *Chem. Eur. J.* **2019**, *25*, 14300–14303.

(36) Bouammali, A.; Coffinet, A.; Vendier, L.; Simonneau, A. Dinitrogen-Derived (Diarylboryl)Diazenido Complexes with Differing Coordination to the Thallium Cation. *Dalton Trans*. **2022**, *51*, 10697–10701.

(37) Coffinet, A.; Zhang, D.; Vendier, L.; Bontemps, S.; Simonneau, A. Borane-catalysed dinitrogen borylation by 1,3-B–H bond addition. *Dalton Trans*. **2021**, *50*, 5582–5589.

(38) Simonneau, A.; Turrel, R.; Vendier, L.; Etienne, M. Group 6 Transition-Metal/Boron Frustrated Lewis Pair Templates Activate N_2 and Allow its Facile Borylation and Silylation. *Angew. Chem. Int. Ed*. **2017**, *56*, 12268–12272.

(39) Rempel, A.; Mellerup, S. K.; Fantuzzi, F.; Herzog, A.; Deißenberger, A.; Bertermann, R.; Engels, B.; Braunschweig, H. Functionalization of N_2 via Formal 1,3-Haloboration of a Tungsten(0) σ-Dinitrogen Complex. *Chem. Eur. J.* **2020**, *26*, 16019–16027.

(40) Haufe, L. C.; Arrowsmith, M.; Dietz, M.; Gärtner, A.; Bertermann, R.; Braunschweig, H. Spontaneous N_2-diboranylation of [W(N_2)$_2$(dppe)$_2$] with $B_2Br_4(SMe_2)_2$. *Dalton Trans.* **2022**, *51*, 12786–12790.

(41) Nöth, H.; Pommerening, H. Beitrage zur Chemie des Bors, 174. Isomerisierung von 2,3-Dihydro-l,4,2,3-dithiadiborin-, 1,4,2,3-Dithiadiborinan- und 2,3-Dihydro-1,4,2,3-benzodithiadiborin-Derivaten. *Chem. Ber*. **1986**, *119*, 2261–2271.

(42) Despite multiple crystallization attempts the X-ray crystallographic data of **1-Mes** remained of insufficient completeness to enable the discussion of structural parameters.

(43) Berski, S.; Latajkaa, Z.; Gordon, A. J. On the multiple B–N bonding in boron compounds using the topological analysis of electron localization function (ELF). *New J. Chem*. **2011**, *35*, 89–96.

(44) Mierzwa, G.; Gordon, A. J.; Berski, S. The nature of multiple boron-nitrogen bonds studied using electron localization function (ELF), electron density (AIM), and natural bond orbital (NBO) methods. *J. Molec. Model.* **2020**, *26*, Article 136.

(45) Danopoulos, A. A.; Redshaw, C.; Vaniche, A.; Wilkinson, G.; Hussain-Bates, B.; Hursthouse, M. B. Organoimido Complexes of Tungsten. X-Ray Crystal Structures of W(NC_6H_{11})$Cl_2(PMe_3)_3$, [W(NC_6H_{11})$Cl_2(PMe_3)_3$]O_3SCF_3, [W(NC_6H_{11})Cl(PMe_3)$_4$]BPh_4, W[NSi(*o*-MeC_6H_4)$_3$]$Cl_2(PMe_3)_3$, W[NB(mes$_2$)]$_2Cl_2(PMe_3)_2$, {W(NPh)Cl[$O_2C_2(CF_3)_4$]$_2$}Li and $WCl_4(PMe_2Ph)_3$. *Polyhedron* **1993**, *12*, 1061–1071.

(46) Bartlett, R. A.; Chen, H.; Dias, H. V. R.; Olmstead, M. M.; Power, P. P. Synthesis and spectroscopic and structural characterization of the novel lithium borylamide salts trans-[Li(Et_2O)NHBMes$_2$]$_2$, a dimer, and the ion pair [Li(Et_2O)$_3$][Mes$_2$BNBMes$_2$] with a linear allene-like, [R_2B=N=BR_2]$^+$ moiety. *J. Am. Chem. Soc.* **1988**, 110, 446–449.

(47) Zhu, L.; Kinjo, R. Single-Nitrogen Atom Incorporation into B=B Bond via the N=N Bond Splitting of Diazo Compound and Diazirine. *Angew. Chem. Int. Ed*. **2023**, *62*, e2023065.

(48) Nöth, H.; Prigge, H. Ein Allen-analoges Diborylamid-Ion. *Chem. Ber*. **1987**, *120*, 907–909.

(49) Braunschweig, H.; Damme, A.; Dewhurst, R. D.; Kramer, T.; Kupfer, T.; Radacki, K.; Siedler, E.; Trumpp, A.; Wagner, K.; Werner, C. Quaternizing Diboranes(4): Highly Divergent Outcomes and an Inorganic Wagner-Meerwein Rearrangement. *J. Am. Chem. Soc.* **2013**, *135*, 8702–8707.

(50) Arnold, N.; Braunschweig, H.; Dewhurst, R. D.; Hupp, F.; Radacki, K.; Trumpp, A. Desymmetrizing Electron-Deficient Diboranes(4): Diverse Products and Their Reactivity. *Chem. Eur. J.* **2016**, *22*, 13927–13934.

(51) We have previously reported that the tribromodiboranyldiazenido complex obtained from the reaction of *trans*-[W(N_2)$_2$(dppe)$_2$] with $B_2Br_4(SMe_2)_2$ (see Scheme 3) proved unstable in solution due to the lability of the SMe_2 ligand. In light of our calculated mechanism, it is highly likely that the complex undergoes a similar rearrangement via an equivalent of **TS3**. The resulting van der Waals complex equivalent of **C**, however, would likely be unstable due to the highly reactive and exposed terminal BBr_2 unit of the iminoborane moiety, which in the BBrAr derivatives is shielded by the bulky aryl group.

(52) Bevan, P. C.; Chatt, J.; Dilworth, J. R.; Henderson, R. A.; Leigh, G. J. The preparation and reactions of azidobis[1,2-bis(diphenylphosphino)-ethane]nitridotungsten(IV). *J. Chem. Soc. Dalton Trans*. **1982**, 821–824.

(53) Finally, it is worth noting that the rearrangement mechanism may encompass not only the isomers shown, but also their rotamers concerning the geometries of **B**, **TS3** and **2-Mes**. In this scenario, the mesityl group and the bromine atom would interchange at the terminal boron atom. Nonetheless, this has a negligible effect on the reaction mechanism. The Gibbs free energies of the resulting isomers **B'**, **TS3'** and **2-Mes'** are –2.0, 25.4, and –62.9 kcal mol^{-1}, respectively. Accordingly, the rate-determining step is also similar in magnitude with a barrier of 27.4 kcal mol^{-1}.

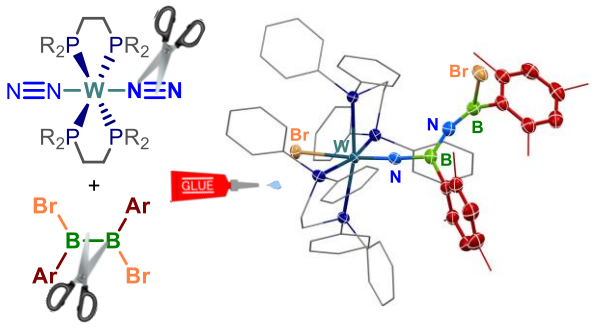
R2P
PR2
N≡N–W–N≡N
R2P
PR2
+
Br
Ar
B–B
Ar
Br
GLUE
Br
W
N
B
N
B
Br